

1
2
3
4 **Selective inhibition of fibroblast-specific Domain Discoidin Receptor 1**
5 **(DDR1) reduces collagen deposition and modulates fibroblast-specific**
6 **cytokine release within the breast microenvironment.**

7
8
9 Daniel E.C. Fein^{1*}, Nicole Traugh², Gat Rauner², Youssof Mal³, Colin Trepicchio²,
10 Charlotte Kuperwasser^{2,3}.

11
12
13 ¹Department of Medicine, Division of Hematology/Oncology, Beth Israel Deaconess
14 Medical Center, Boston, MA

15 ²Department of Cell, Molecular, & Developmental Biology, Tufts Graduate School of
16 Biomedical Sciences, Boston, MA, USA

17 ³Department of Genetics, Tufts Graduate School of Medical Biosciences, Boston, MA,
18 USA

19
20
21 *Corresponding author
22 Email: dfein@bidmc.harvard.edu

23 **Abstract**

24 Fibroblasts are a major cell type within breast microenvironment which play key roles in
25 tissue remodeling during the processes of normal development, injury, and malignancy.
26 During wound healing and tumorigenesis, fibroblasts facilitate production and
27 degradation of the extracellular matrix and produce inflammatory mediators which act as
28 immune regulators. Domain Discoidin Receptor 1 (DDR1) is a cell surface tyrosine kinase
29 receptor expressed by epithelial and stromal cells which is activated by collagen. In the
30 breast, DDR1 expression and activity has been implicated in the development of fibrosis
31 as well as chemotherapy resistance. We set out to examine whether selective inhibition
32 of DDR1 would modulate fibroblast immunomodulatory function to generate an immune-
33 permissive breast microenvironment and reduce stromal desmoplasia. In vivo, DDR1
34 inhibition resulted in mammary fibroblast tissue remodeling, reduced collagen deposition,
35 and changes in immunomodulatory cytokine expression. Furthermore, DDR1 inhibition
36 was associated with increased CD45.2+ immune cell infiltration and reduced
37 Ly6G+/Ly6C- neutrophil infiltration. Mechanistically, we developed an ex-vivo 3D collagen
38 hydrogel model of desmoplasia to study the effects of DDR1 inhibition on the expression
39 of immune modulating factors and fibroblast functions and features. We found that DDR1
40 regulates the expression and secretion of key immunomodulatory cytokines (IL-6, IL-8,
41 and MCP-1). Collectively these findings suggest that breast fibroblast-specific DDR1
42 mediates collagen deposition and immunomodulatory function within the mammary gland
43 and warrants further investigation as a potential target for fibroblast-modulating therapy
44 in benign and neoplastic breast disorders.

45 **Introduction**

46 The fibroblast is the principal cell that synthesizes collagen and extracellular matrix of the
47 mammary stroma. Now considered a major participant in the mammary immune
48 response, fibroblasts have emerged as a new target for treatment of benign and
49 neoplastic breast disorders given their contribution to desmoplasia, tumor growth,
50 metastasis, and suppression of the anti-tumor immune response¹⁻⁴. Fibroblasts activate
51 in response to stress and pathological conditions by transitioning to a contractile
52 phenotype as such^{1,5}. This process is referred to as desmoplasia.

53 In the breast, cancer-associated fibroblasts (CAFs) are predominantly formed from
54 conversion of tissue-resident mammary fibroblasts through varied mechanisms including
55 increasing extracellular matrix (ECM) stiffness, ECM composition, hypoxia, and
56 overproduction of activating signals such as TGF β and IL-6^{1,6-8}. The clinical experience
57 in targeting CAFs has been limited and in some instances has resulted in paradoxically
58 increased tumor aggressiveness^{2,9,10}. As a result, there has been a call for further
59 understanding of the relation of fibroblast markers to function as well as to prioritize
60 strategies aimed to reprogram CAFs rather than ablate them¹¹.

61 Domain Discoidin Receptor 1 (DDR1) is a cell surface tyrosine kinase receptor expressed
62 by epithelial and stromal cells which is activated by collagen within the breast
63 microenvironment¹²⁻¹⁴. DDR1 has been identified as a key mediator of the stromal-
64 epithelial interactions during ductal morphogenesis in the human mammary gland^{15,16}. In
65 breast cancer, DDR1 expression has been associated with desmoplasia, chemotherapy
66 resistance, tumor invasiveness, and metastasis of yet unclear mechanisms^{13,17-20}. Most
67 recently, tumor DDR1 has been implicated in immune cell exclusion through a mechanism
68 of collagen fiber realignment within the TME²¹. The effects of pharmacologic targeting of
69 DDR1-dependent stromal-epithelial interactions on the desmoplastic response and
70 immune cell composition remain unclear. In this study, we set out to study how
71 desmoplasia may affect an immunological response by examining whether selective
72 inhibition of DDR1 would affect fibroblast immunomodulatory function. In doing so, we
73 found that inhibiting collagen signaling can generate an immune-permissive breast
74 microenvironment and reduce stromal desmoplasia within the benign mammary gland.

75 **Results**

76 **DDR1 inhibition reduces collagen deposition and modulates expression of** 77 **inflammatory cytokines and markers of ECM remodeling**

78 Fibroblast release of immunomodulatory cytokines has been implicated as a driver of the
79 desmoplastic response through numerous cell-dependent and independent interactions¹.
80 These interactions may be context dependent, in that the stromal secretome may be
81 influenced by the composition and stiffness of the surrounding ECM¹. To study the role
82 of mammary fibroblasts connection between role of DDR1 on the mammary stroma,

83 extracellular matrix remodeling, cytokine profile, and immune cell composition, we treated
84 12-week-old C57Bl/6 female mice with an inhibitor of DDR1 (Fig 1A). Mice were
85 administered an orally bioavailable selective DDR1 inhibitor (DDRi) once daily for 14
86 days, after which thoracic and inguinal mammary glands (#2-3 and #4-5, respectively)
87 were collected and examined. Picosirius red staining of inguinal mammary glands after
88 treatment showed a reduction in collagen content within the mammary tissue (Fig 1B,
89 1C). Gene expression analysis showed reduced expression of markers of ECM
90 remodeling in the DDR1i group including collagen type 1 (*Col1a1*), collagen type 4
91 (*Col4a1*), and *Mmp9* (Fig 1E).

92 Given the reduction in immunomodulatory cytokine expression and collagen content in
93 mammary tissues, we examined the immune cell composition of the mammary gland.
94 Using an established immunophenotyping panel²⁸, multiplexed flow cytometry of inguinal
95 mammary glands was performed to assess the innate and adaptive immune cell
96 compositions (Fig S1, Fig S2). We observed trends in increased CD45.2+ hematopoietic
97 cell percentage in the DDR1i group (Fig 2A). Also observed in the DDR1i group were
98 trends in reduced CD11b+ myeloid and CD11b+Ly6G+Ly6C- neutrophil populations (Fig
99 2A). The relative percentage of CD11b+Ly6G-Ly6C- macrophages were increased. The
100 total percentage of CD19+TCR β - B cells and CD19-TCR β + T cells were increased in the
101 DDR1i group (Fig 2B). Consistent with findings in the mammary stroma, the spleen also
102 showed a significant reduction in the CD11b+Ly6G+Ly6C- neutrophil population and a
103 significant increase in CD11b+Ly6G-Ly6C- macrophage population (Fig 3A). Associated
104 with reduction in neutrophil population, we observed reduced gene expression of potent
105 chemokines *Cxcl1* and *Cxcl12* (Fig 1D) in the mammary gland. In association with the
106 trends of increased macrophage infiltration seen (Fig 2A, 3A), trends in increased *Cxcl2*
107 expression were also observed in the mammary glands of the DDR1i group (Fig 1D).

108 **Collagen concentration and cell density have an important role in the contraction
109 and expression of immune modulating factors by mammary fibroblasts**

110 To study how DDR1i leads to changes in stromal collagen, we characterized the effect of
111 ECM and cell density on the expression of key cytokines previously identified as drivers
112 of tumor growth, metastasis, and modulators of the immune microenvironment²²⁻²⁵.

113 Immortalized human breast tissue fibroblasts obtained from reduction mammoplasty
114 tissue (RMF-EG fibroblasts³¹) were seeded into 3D collagen-I gels at increasing stiffness
115 and cell density (Fig 4A). Fibroblasts in low stiffness gels exhibited increased contraction
116 (Fig 4A). Additionally, fibroblasts in the fully contracted gels were observed to upregulate
117 pro-inflammatory cytokines including *IL6* and *IL1b* (Fig 4B). By increasing cell density, a
118 modest increase in collagen gel contraction was observed (Fig 4C). However, this modest
119 increase in gel contraction was associated with marked upregulation of *IL6* and *IL1b* (Fig
120 4D). This may suggest that the pro-inflammatory secretome of mammary fibroblasts is
121 regulated significantly by both cell density as well as ECM stiffness and composition.
122 Given these observations, we hypothesized that interruption of cell-ECM interactions
123 through selective DDR1 inhibition could reprogram mammary fibroblast ECM remodeling
124 and immune modulating functions.

125 **Selective DDR1 inhibition modulates human fibroblast expression of**
126 **cytokines and markers of ECM remodeling in vitro**

127 We next sought to characterize the changes in fibroblast cytokine expression profile
128 induced by DDR1i. RMF-EG were seeded into collagen gels with or without the addition
129 of selective DDR1 tyrosine kinase inhibitors^{26,27}. With DDR1i we observed significant
130 reduction in RMF-EG-mediated collagen gel contraction (Fig 5A) in association with
131 reduced DDR1 phosphorylation (Fig S3). Reduced expression of CAF markers *αSMA*
132 and *FAP* were seen with DDR1i, in addition to marked reduction in *IL6* expression (Fig
133 5B). Conditioned media from RMF-EG fibroblasts cultured in 3D was collected for
134 multiplex human cytokine array analysis. We identified elevated expression of cytokines
135 *IL-6*, *IL-8*, and *MCP-1* which were reduced with DDR1i (Fig 5C). No significant difference
136 in *IL-1b* was observed (Fig 5C). Associated with reduced cytokine secretion, reduced
137 mRNA expression of *IL6*, *IL8*, and *MCP1* with DDR1i was observed (Fig 5C,D).
138 Interestingly, we observed that the relative reduction in mRNA expression of *IL6*, *IL8*, and
139 *MCP1* was enhanced in RMF-EG grown in 3D collagen gels compared to those grown in
140 2D. In assessing genetic markers of ECM remodeling, we observed upregulation of
141 collagen type 1 (*Col1a1*) and matrix metalloproteases (*Mmp9*) in RMF-EG cultured in the
142 presence of collagen; DDR1i-induced downregulation of *Col1a1* and *Mmp9* was seen
143 only in the 3D context (Fig 5D). Additionally, when stimulated to a myofibroblast

144 phenotype with prolonged TGF β 1 treatment, RMF-EG fibroblasts were noted to have
145 significant downregulation of *IL6* and α SMA when cultured in either 2D or 3D (Fig S5). To
146 correlate these findings with our *in vivo* studies, we assessed mRNA expression of key
147 cytokines in the mouse mammary gland, observing trends reduction of *IL6*, collagen, and
148 matrix metalloprotease expression in the DDR1i treated mice compared with vehicle (Fig
149 1E).

150 **Discussion**

151 Investigations of fibroblast reprogramming in efforts to alter the disease course of fibrotic
152 and malignant breast conditions have been limited by the 2D culture context. Using 3D
153 culture models, one may more accurately emulate the composition and stiffness of the
154 tissue microenvironment, factors known to significantly impact the proteome of supportive
155 stromal cells²⁹. Using a 3D collagen type I hydrogel model, we demonstrated the impact
156 of breast fibroblast cell density, collagen density, and collagen gel contraction on the
157 expression of potent immunomodulatory cytokines and subsequently the impact of
158 interrupting stromal-ECM interactions through DDR1i. As stromal-collagen signaling
159 through DDR1 has been implicated in the development of desmoplasia, treatment
160 resistance, and tumor invasiveness, we hypothesized that modulation of the breast
161 fibroblast secretome through DDR1 could reduce collagen deposition within the
162 mammary gland.

163 In a DDR1 knockout (KO) animal model, it was observed that deletion of DDR1 reduced
164 the growth of transplanted DDR1-intact murine mammary tumors and altered extracellular
165 matrix remodeling of the tumor microenvironment³⁰. Screening of the stromal fraction
166 secretome identified IL-6 as a cytokine which was secreted in a DDR1-dependent
167 manner, a mechanism subsequently implicated in accelerating tumor cell invasion and
168 growth *in vivo*. These findings suggested that stromal cell-specific production of soluble
169 factors such as IL-6 are functionally linked to DDR1 activity in the stromal compartment
170 and are sufficient to accelerate breast cancer growth and aggressiveness³⁰.

171 Accordingly, using small molecular DDR1 inhibitors, we observed downregulation and
172 reduced secretion of breast fibroblast-specific IL-6 amongst other key immunomodulatory

173 cytokines including IL-8 and MCP-1. We noted an enhanced effect of IL-6 reduction when
174 fibroblasts were cultured in 3D collagen-I gels, suggesting a context-dependent
175 mechanism of DDR1 signaling which is enhanced in a collagen-rich environment.
176 Treatment of mice with DDR1i resulted in downregulation of IL-6 within the benign
177 mammary gland. This finding was associated with downregulation of type 1 and 4
178 collagens as well as reduced collagen deposition. These findings support the existing
179 evidence which have correlated DDR1 signaling activity with ECM-remodeling within the
180 mammary gland.

181 A novel mechanism of tumor cell-mediated immune cell exclusion facilitated by DDR1-
182 dependent collagen fiber realignment within the TME was recently uncovered²¹. In this
183 study, DDR1-KO breast tumors implanted into DDR1-intact immunocompetent hosts
184 were found to have increased CD4+ and CD8+ T cell infiltration with reduced tumor
185 growth in association. This finding was not observed in immunodeficient hosts,
186 suggesting a key role of DDR1 in regulating the adaptive immune system response to
187 tumor growth. The binding of the DDR1 extracellular domain (DDR1-ECD) to collagen
188 fibers was implicated in the enforcement of a stromal barrier contributing to the immune
189 cell exclusion seen²¹.

190 We thus characterized the lymphoid and myeloid immune cell populations within the
191 benign mammary glands of mice treated with or without DDR1i and observed increased
192 infiltration of CD45.2+ immune cells, CD19+ B cells, and TCR β + T cells with DDR1i.
193 These findings contribute to existing evidence supporting the role stromal-cell specific
194 DDR1 signaling in regulation of the immune cell composition of the mammary gland. In
195 addition to interruption of DDR1-ECD-dependent collagen realignment, our findings
196 suggest that DDR1 inhibition may further modify ECM remodeling through reduced
197 production of collagens and matrix metalloproteases.

198 This study had limitations. Our *in vitro* studies do not fully address the impact of DDR1 on
199 the modification of associated mechanotransduction signaling pathways (e.g. TNF α /NF- κ B,
200 integrin, Rho GTPase-activating protein signaling), although our preliminary studies
201 have not suggested TNF α /NF- κ B to be implicated (Fig S6). We did not assess the impact
202 of DDR1i *in vivo* in the context of induced desmoplasia, however, the reductions in α SMA

203 and *IL6* expression observed in the TGF β -induced myofibroblast phenotype (Fig S5)
204 suggest potent activity of DDR1i in that context. *In vivo*, we did identify similar alterations
205 of immune cell populations within the spleen, however, we did not assess further the
206 systemic effects of DDR1i as it relates to chemokine expression and collagen deposition
207 within other tissues.

208 In summary, these findings suggest that disruption of fibroblast-ECM signaling through
209 DDR1 inhibition may be a novel strategy to reprogram the desmoplasia-inducing and
210 tumor-promoting features of mammary fibroblasts. Further studies are warranted to
211 assess the immune-modulating capability and anti-tumor activity of selective DDR1
212 inhibition in benign and malignant breast disorders.

213

214 Materials and Methods:

215 **Cell Culture and 3D collagen hydrogel formation:** Immortalized human mammary
216 fibroblasts, RMF-EG, were initially derived from primary human breast fibroblasts
217 obtained from reduction mammoplasty tissues as described previously³¹. RMF-EG were
218 cultured in DMEM (Corning 10017CV) with 10% FBS (Gibco) and 1%
219 antibiotic/antimycotic (Corning MT30004CL). Collagen hydrogel 3D culture and
220 contraction assays were performed as described previously³². Briefly, RMF-EG were
221 seeded in rat tail collagen type 1 (Millipore Sigma 08115) hydrogels at varied cell number
222 and collagen concentrations in 24 well ultra-low attachment surface plates (Corning
223 3473). Media without or without DDR1 inhibitor (DDR1-IN-1 [Tocris 5077] or 7rh [Tocris
224 5860] was added and gel contraction quantified at 8-16 hours. For collagen stimulation
225 assays, RMF-EG were seeded into 6 well tissue culture plates (Corning 3516) with or
226 without the addition of rat tail collagen type I to a final concentration of 0.05 mg/mL. For
227 the TGF β 1 activation assays, RMF-EG 100,000 cells were seeded in 500 μ L collagen I
228 gels (1mg/mL) or on tissue culture plate, exposed to recombinant human TGF β 1 (Thermo
229 Fisher 7754BH005) 2ng/ml for 3 days, followed by treatment with DDR1i 1 μ M for 24
230 hours.

231 **RNA extraction and RT-qPCR:** Total RNA was isolated using TRIzol reagent
232 (ThermoFisher 15596026) and RNeasy Mini Kit (Qiagen 74106). cDNA synthesis was
233 performed using the iScript cDNA synthesis kit (Bio-Rad 1708891). qPCR assays were
234 performed with the CFX Connect Real-Time PCR detection system (Bio-Rad) and iTaq
235 Universal SYBR Green SuperMix (Bio-Rad 1725124). Each condition for the tested genes
236 were repeated three times in triplicate. Gene expression analysis was performed using
237 ddCq method with relative gene expression normalized to that of *GAPDH*. Mouse primer
238 pairs used: *IL6* F-ACAAAGCCAGAGTCCTCAGAG, R-
239 GTGAGGAATGTCCACAAACTGA; *MCP1*: F-TTTTGTCAACCAAGCTCAAGAGA; R-
240 ATTAAGGCATCACAGTCCGAGT; *GAPDH* F-GATGACATCAAGAAGGTGGTG; R-
241 GGTCCAGGGTTCTTACTCCTT; *Mmp9* F-CAGCCGACTTTGTGGTCTTC; R-
242 CGGTACAAGTATGCCTCTGCCA; *Col1a1* F-CCCTGGTCCCTCTGGAAATG; R-
243 GGACCTTGCCCCCTTCTT, *Col1a4* F-AAAGGCTCTCCGGGTTCAAT, R-
244 CCGATGTCTCCACGACTAC; *Cxcl1* F-CCCAAACCGAAGTCATAGCCA, R-
245 CTCCGTTACTTGGGGACACC; *Cxcl12* F-CCTTCAGATTGTTGCACGGC; R-
246 CTTGCATCTCCCACGGATGT. Human primer pairs used: *SMA* F-
247 CAGGGCTGTTTCCCATCCAT, R-GCCATGTTCTATCGGGTACTTC; *FAP* F-
248 AATGAGAGCACTCACACTGAAG, R-CCGATCAGGTGATAAGCCGTAAT; *IL6* F-
249 AAGCCAGAGCTGTGCAGATGAGTA, R-TGTCCTGCAGCCACTGGTTC; *GAPDH* F-
250 GAGTCAACGGATTGGTCGT, R-TTGATTTGGAGGGATCTCG; *IFNG* F-
251 TCGGTAACTGACTTGAATGT, R-TCGCTCCCTGTTTAGCTC; *COL1A1* F-
252 GACAGAGGCTACAAGGTGAA, R-GTGGACCCATAGGACCGATG; *IL6* F-
253 AAGCCAGAGCTGTGCAGATGA, R-TGTCCTGCAGCCACTGGTTC; *IL1B* F-
254 CTCGCCAGTGAAATGATGGCT, R-GTCGGAGATTCTGTAGCTGGAT; *IL8* F-
255 TTTGCCAAGGAGTGCTAAAGA, R-AACCCTCTGCACCCAGTTTC; *MCP1* F-
256 GAGAGGCTGAGACTAACCCAGA, R-ATCACAGCTTCTTGGGACACT,

257

258 **Multiplex Cytokine Array:** Conditioned media was generated by culturing RMF-EG in
259 3D hydrogels for 72 hours followed by the addition of serum free DMEM for 24 hours. Cell
260 supernatants were centrifuged at 300g x 5 mins, filtered using a 0.22 μ m membrane filter,

261 and stored at -80C. Cytokine profiling of cell supernatants was performed using Human
262 Cytokine Array C5 (RayBiotech AAH-CYT-5-2) and imaged using the ChemiDoc MP
263 Imaging system (Bio-Rad). Relative protein expression was determined per manufacturer
264 recommendations.

265 **In Vivo:** Eight-week-old female C57BL/6J mice (Jackson Laboratories) were administered
266 7rh DDR1 inhibitor (Tocris 5860) 25 mg/kg or vehicle control (1% carboxymethylcellulose
267 [Fisher Scientific C5678], 0.25% Tween 80 [Millipore Sigma P1754]) via oral gavage for
268 14 days. Mice were sacrificed followed by collection of inguinal/thoracic mammary glands
269 and spleens for RT-qPCR, immunohistochemistry, and flow cytometry analysis. Inguinal
270 lymph nodes were dissected away from inguinal mammary glands prior to RNA extraction
271 and single cell suspension formation. RNA was extracted using a TissueLyser LT
272 (Qiagen) and RNEasy MiniKit (Qiagen 74106), with RT-qPCR performed as described
273 above. Inguinal mammary glands were fixed in 10% neutral buffered formalin (Millipore
274 Sigma HT501128) followed by paraffin-embedding and picrosirius red staining as
275 performed by the Tufts Animal Histology Core. Collagen deposition was assessed by
276 quantifying the amount of picrosirius red staining in a minimum of 8 fields at 10x objective
277 for each mammary gland section using ImageJ software, version 1.52a³³.

278 **Flow cytometry:** To form single cell suspensions for flow cytometry analysis, mammary
279 glands were finely chopped and digested for 30-60 minutes at 37°C using a using a
280 digestion mixture of collagenase 1.5 mg/mL and hyaluronidase 125 unit/mL in DMEM/F12
281 (Corning MT10090CV), 5% FBS (Gibco), insulin 10 µg/mL (Millipore Sigma I3536),
282 mouse endothelial growth factor 5ng/mL (Millipore Sigma E5160), and hydrocortisone 0.5
283 µg/mL (Millipore Sigma), followed by the addition of RBC lysis buffer (HybriMax Sigma
284 R7757), TrypLE Express Enzyme (Gibco 12604013), and DNase 0.1 mg/mL (Roche
285 1010415900). To form single cell suspensions from spleens, a mechanical digestion
286 method was used. Spleens were homogenized using a 100µm strainer followed by the
287 addition of RBC lysis buffer. The digestion mixturex were filtered through 100 µm and 40
288 µm filters and suspended in 1% BSA (Rockland BSA50) and 1 mM EDTA in phosphate
289 buffered saline. Cells were incubated for 30 minutes at 4°C with myeloid or lymphoid
290 antibody panels as previously described²⁸; the following antibodies were used: CD45.2-

291 APC-Cy7 (BioLegend 109823; 1:200), CD11b-PE (BioLegend 101207; 1:2400), CD11c-
292 APC (BD 561119; 1:400), Ly6C-BV421 (BD 562727; 1:800), Ly6G-PE-Cy7 (BioLegend
293 127617; 1:2400), CD206-FITC (BioLegend 141703; 1:800), CD49b-FITC (BD 561067;
294 1:800), CD45.2-PE (BioLegend 109807; 1:400), TCR β -PE-Cy7 (BioLegend 109221;
295 1:400), CD19-APC (BioLegend 115511; 1:800), CD8-BV711 (BioLegend 100747; 1:800),
296 CD4-APC-Cy7 (BioLegend 100413; 1:400). Propidium iodide (1:5000) was added to each
297 antibody panel for viability assessment. Flow cytometry was performed on a BD LSR-II
298 flow cytometer at the Tufts Flow Cytometry Core. UltraComp eBeads Plus Compensation
299 Beads (Invitrogen 01333341) were used for single-color compensation controls. Flow
300 cytometry data were collected using FACS Diva, version 6.2. Flow cytometry
301 compensation and data analysis was performed on FlowJo software v10.7.1. All analyses
302 were performed in compliance with MiFlowCyt standards³⁴.

303 **Acknowledgments**

304 We gratefully acknowledge Tufts Comparative Medicine Services (CMS) for *in vivo*
305 supportive services. We thank Nathan Li of Tufts Animal Histology Core for tissue
306 processing and special stains. We thank Stephen Kwok and Allen Parmelee of the Tufts
307 University Flow Cyometry Core for assistance with flow cytometry analysis. This
308 research was supported by the Breast Cancer Research Foundation.

309 **References**

- 310 1. Kalluri R. The biology and function of fibroblasts in cancer. *Nat Rev Cancer*.
311 2016;16(9):582-598. doi:10.1038/nrc.2016.73
- 312 2. Liu T, Han C, Wang S, et al. Cancer-associated fibroblasts: An emerging target of anti-
313 cancer immunotherapy. *J Hematol Oncol*. 2019;12(1):86. doi:10.1186/s13045-019-0770-
314 1
- 315 3. Gieniec KA, Butler LM, Worthley DL, Woods SL. Cancer-associated fibroblasts—heroes
316 or villains? *Br J Cancer*. 2019;121(4):293-302. doi:10.1038/s41416-019-0509-3
- 317 4. De Jaeghere EA, Denys HG, De Wever O. Fibroblasts Fuel Immune Escape in the Tumor
318 Microenvironment. *Trends in Cancer*. 2019;5(11):704-723.
319 doi:10.1016/j.trecan.2019.09.009

320 5. Nurmik M, Ullmann P, Rodriguez F, Haan S, Letellier E. In search of definitions: Cancer-
321 associated fibroblasts and their markers. *Int J Cancer*. 2020;146(4):895-905.
322 doi:10.1002/ijc.32193

323 6. Wu SZ, Roden DL, Wang C, et al. Stromal cell diversity associated with immune evasion
324 in human triple-negative breast cancer. *EMBO J*. Published online August 13, 2020.
325 doi:10.15252/embj.2019104063

326 7. Conklin MW, Keely PJ. Why the stroma matters in breast cancer: Insights into breast
327 cancer patient outcomes through the examination of stromal biomarkers. *Cell Adhes
328 Migr*. 2012;6(3):249-260. doi:10.4161/cam.20567

329 8. Kojima Y, Acar A, Eaton EN, et al. Autocrine TGF- β and stromal cell-derived factor-1
330 (SDF-1) signaling drives the evolution of tumor-promoting mammary stromal
331 myofibroblasts. *Proc Natl Acad Sci U S A*. 2010;107(46):20009-20014.
332 doi:10.1073/pnas.1013805107

333 9. Rhim AD, Oberstein PE, Thomas DH, et al. Stromal elements act to restrain, rather than
334 support, pancreatic ductal adenocarcinoma. *Cancer Cell*. 2014;25(6):735-747.
335 doi:10.1016/j.ccr.2014.04.021

336 10. Özdemir BC, Pentcheva-Hoang T, Carstens JL, et al. Depletion of carcinoma-associated
337 fibroblasts and fibrosis induces immunosuppression and accelerates pancreas cancer
338 with reduced survival. *Cancer Cell*. 2014;25(6):719-734. doi:10.1016/j.ccr.2014.04.005

339 11. Sahai E, Astsaturov I, Cukierman E, et al. A framework for advancing our understanding
340 of cancer-associated fibroblasts. *Nat Rev Cancer*. 2020;20(3):174-186.
341 doi:10.1038/s41568-019-0238-1

342 12. Moll S, Desmoulière A, Moeller MJ, et al. DDR1 role in fibrosis and its pharmacological
343 targeting. *Biochim Biophys Acta - Mol Cell Res*. 2019;1866(11):118474.
344 doi:10.1016/j.bbamcr.2019.04.004

345 13. Jing H, Song J, Zheng J. Discoidin domain receptor 1: New star in cancer-targeted
346 therapy and its complex role in breast carcinoma (review). *Oncol Lett*. 2018;15(3):3403-
347 3408. doi:10.3892/ol.2018.7795

348 14. Leitinger B. Transmembrane Collagen Receptors. *Annu Rev Cell Dev Biol*.
349 2011;27(1):265-290. doi:10.1146/annurev-cellbio-092910-154013

350 15. Vogel W, Gish GD, Alves F, Pawson T. The Discoidin Domain Receptor Tyrosine
351 Kinases Are Activated by Collagen. *Mol Cell*. 1997;1(1):13-23. doi:10.1016/S1097-
352 2765(00)80003-9

353 16. Rauner G, Jin DX, Miller DH, et al. Breast tissue regeneration is driven by cell-matrix
354 interactions coordinating multi-lineage stem cell differentiation through DDR1. *Nat
355 Commun*. 2021;12(1):7116. doi:10.1038/S41467-021-27401-6

356 17. Das S, Ongusaha PP, Yang YS, Park JM, Aaronson SA, Lee SW. Discoidin domain
357 receptor 1 receptor tyrosine kinase induces cyclooxygenase-2 and promotes
358 chemoresistance through nuclear factor- κ B pathway activation. *Cancer Res*.
359 2006;66(16):8123-8130. doi:10.1158/0008-5472.CAN-06-1215

360 18. Castro-Sanchez L, Soto-Guzman A, Guaderrama-Diaz M, Cortes-Reynosa P, Salazar
361 EP. Role of DDR1 in the gelatinases secretion induced by native type IV collagen in
362 MDA-MB-231 breast cancer cells. *Clin Exp Metastasis*. 2011;28(5):463-477.
363 doi:10.1007/s10585-011-9385-9

364 19. Gao H, Chakraborty G, Zhang Z, et al. Multi-organ Site Metastatic Reactivation Mediated
365 by Non-canonical Discoidin Domain Receptor 1 Signaling. *Cell*. 2016;166(1):47-62.
366 doi:10.1016/j.cell.2016.06.009

367 20. Zhong X, Zhang W, Sun T. DDR1 promotes breast tumor growth by suppressing
368 antitumor immunity. *Oncol Rep*. 2019;42(6):2844-2854. doi:10.3892/or.2019.7338

369 21. Sun X, Wu B, Chiang H-C, et al. Tumour DDR1 promotes collagen fibre alignment to
370 instigate immune exclusion. *Nature*. 2021;599(7886):673-678. doi:10.1038/s41586-021-
371 04057-2

372 22. Fisher DT, Appenheimer MM, Evans SS. The two faces of IL-6 in the tumor
373 microenvironment. *Semin Immunol*. 2014;26(1):38-47. doi:10.1016/j.smim.2014.01.008

374 23. Tulotta C, Lefley D V., Moore CK, et al. IL-1B drives opposing responses in primary
375 tumours and bone metastases; harnessing combination therapies to improve outcome in
376 breast cancer. *npj Breast Cancer*. 2021;7(1):95. doi:10.1038/s41523-021-00305-w

377 24. Yang F, Takagaki Y, Yoshitomi Y, et al. Inhibition of Dipeptidyl Peptidase-4 Accelerates
378 Epithelial–Mesenchymal Transition and Breast Cancer Metastasis via the
379 CXCL12/CXCR4/mTOR Axis. *Cancer Res*. 2019;79(4):735-746. doi:10.1158/0008-

380 5472.CAN-18-0620

381 25. Chen DS, Mellman I. Elements of cancer immunity and the cancer-immune set point.
382 *Nature*. 2017;541(7637):321-330. doi:10.1038/nature21349

383 26. Kim H-G, Tan L, Weisberg EL, et al. Discovery of a Potent and Selective DDR1 Receptor
384 Tyrosine Kinase Inhibitor. *ACS Chem Biol*. 2013;8(10):2145-2150.
385 doi:10.1021/cb400430t

386 27. Gao M, Duan L, Luo J, et al. Discovery and Optimization of 3-(2-(Pyrazolo[1,5- a
387]pyrimidin-6-yl)ethynyl)benzamides as Novel Selective and Orally Bioavailable Discoidin
388 Domain Receptor 1 (DDR1) Inhibitors. *J Med Chem*. 2013;56(8):3281-3295.
389 doi:10.1021/jm301824k

390 28. Unsworth A, Anderson R, Haynes N, Britt K. OMIP-032: Two multi-color
391 immunophenotyping panels for assessing the innate and adaptive immune cells in the
392 mouse mammary gland. *Cytometry A*. 2016;89(6):527-530. doi:10.1002/cyto.a.22867

393 29. Tölle RC, Gaggioli C, Dengjel J. Three-Dimensional Cell Culture Conditions Affect the
394 Proteome of Cancer-Associated Fibroblasts. *J Proteome Res*. 2018;17(8):2780-2789.
395 doi:10.1021/acs.jproteome.8b00237

396 30. Sun X, Gupta K, Wu B, et al. Tumor-extrinsic discoidin domain receptor 1 promotes
397 mammary tumor growth by regulating adipose stromal interleukin 6 production in mice. *J
398 Biol Chem*. 2018;293(8):2841-2849. doi:10.1074/jbc.RA117.000672

399 31. Kuperwasser C, Chavarria T, Wu M, et al. Reconstruction of functionally normal and
400 malignant human breast tissues in mice. *Proc Natl Acad Sci U S A*. 2004;101(14):4966-
401 4971. doi:10.1073/pnas.0401064101

402 32. Ngo P, Ramalingam P, Phillips JA, Furuta GT. Collagen gel contraction assay. *Methods
403 Mol Biol*. 2006;341:103-109. doi:10.1385/1-59745-113-4:103

404 33. Schneider CA, Rasband WS, Eliceiri KW. NIH Image to ImageJ: 25 years of image
405 analysis. *Nat Methods*. 2012;9(7):671-675. doi:10.1038/nmeth.2089

406 34. Lee JA, Spidlen J, Boyce K, et al. MIFlowCyt: the minimum information about a Flow
407 Cytometry Experiment. *Cytometry A*. 2008;73(10):926-930. doi:10.1002/cyto.a.20623

408 **Supporting Information**

409

Figure Captions: Fibroblast Domain Discoidin Receptor 1 modulates collagen and cytokine release within the breast.

Corresponding Author: Daniel E.C. Fein, dfein@bidmc.harvard.edu

Figure 1 - Effect of selective DDR1 inhibition (DDR1i) *in vivo* on collagen deposition, extracellular matrix (ECM) remodeling, and inflammatory cytokine expression within the mammary gland.

Twenty 12-week-old C57BL/6J female mice were randomized in 1:1 fashion to receive either DDR1i (7rh 25 mg/kg once daily) or vehicle (1% carboxymethylcellulose, 0.25% Tween 80) via oral gavage for 14 days, followed by sacrifice and immediate collection of mammary glands (A). Picosirius red staining was performed on paraffin-embedded inguinal mammary glands (B), followed by quantification of staining to assess collagen deposition (C). Total RNA was extracted from thoracic mammary glands followed by RT-qPCR gene expression analysis to assess the relative expression of relevant inflammatory chemokines, cytokines, and markers of ECM remodeling (D,E.). * p <0.05, ns - not statistically significant.

Figure 2 - Selective DDR1i *in vivo* modulates the immune cell composition of the mammary gland. Murine inguinal mammary glands were harvested immediately after sacrifice and used to form single cell suspensions through a 1-hour collagenase/hyaluronidase/TrypLE digestion method. This was followed by immediate assessment of myeloid (A) and lymphoid (B) cell populations using a multiplexed flow cytometry approach (Figure S1, S2). ns - not statistically significant.

bioRxiv preprint doi: <https://doi.org/10.1101/2017.08.24.157097>; this version posted August 24, 2017. The copyright holder for this preprint (which was not certified by peer review) is the author/funder, who has granted bioRxiv a license to display the preprint in perpetuity. It is made available under aCC-BY 4.0 International license.

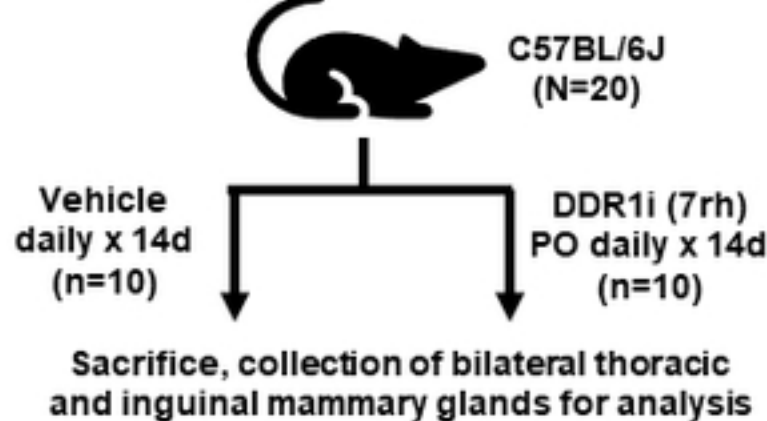
Figure 3 - Selective DDR1i *in vivo* modulates the immune cell composition of the spleen. Murine spleens were harvested immediately after sacrifice and used to form single cell suspensions through a mechanical digestion method. This was followed by immediate assessment of myeloid (A) and lymphoid (B) cell populations using a multiplexed flow cytometry approach (Figure S1, S2). * p <0.05, ns - not statistically significant.

Figure 4 - Immunomodulatory cytokine expression of human mammary fibroblasts *in vitro* is influenced by collagen and cell density. Human mammary fibroblasts (RMF-EG) were seeded into 3D collagen hydrogels at increasing collagen concentration, with increased gel contraction observed at lower collagen gel concentration (A). RNA was isolated from fibroblast-laden gels followed by assessment of relative gene expression of pro-inflammatory cytokines via RT-qPCR analysis, with observation of increased *IL-6* and *IL-1b* expression in gels with lowest collagen concentration/highest gel contraction (B). Increasing fibroblast cell concentration only partially improves gel contraction (C), while *IL-6* and *IL-1b* expression is increased. * p<0.05, ** p<0.01, *** p<0.001 , **** p<0.0001.

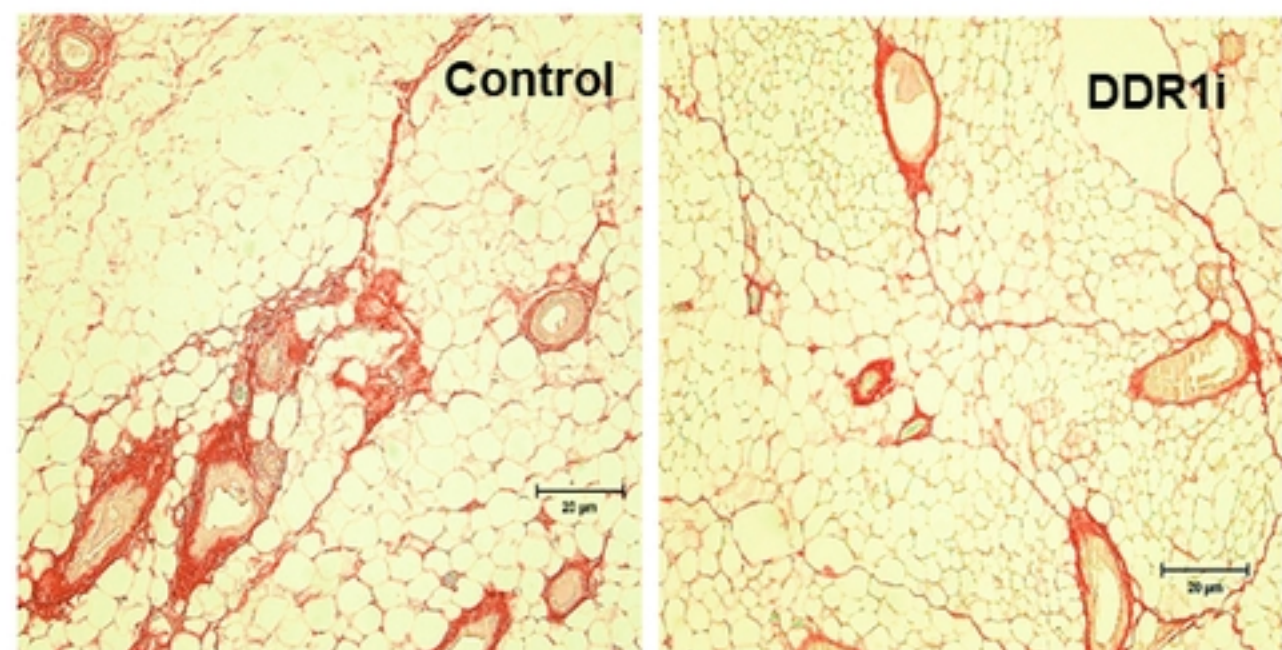
Figure 5 - Selective DDR1i of human mammary fibroblasts cultured in 3D collagen hydrogels reduces expression of inflammatory cytokines and markers of fibroblast function. RMF-EG were cultured in 3D collagen gels in the presence of DDR1i (+) or vehicle (-) followed by assessment of collagen gel contraction [n=3 gels per condition] (A). Reduced gel contraction with DDR1i was observed (A). RMF-EG were cultured on collagen-coated tissue culture plate or in 3D hydrogel, followed by RNA isolation. RT-qPCR gene expression analysis demonstrated that DDR1 inhibition reduces expression of CAF markers *SMA*, *FAP* in the 2D or 3D context (B). *IL-6* was upregulated in RMF-EG cultured in 3D and downregulated with DDR1 inhibition (B). Cell supernatants from RMF-EG laden collagen gels were collected for multiplex human cytokine array analysis. We identified high secretion of IL-6, MCP-1, and IL-8 which were reduced with DDR1 inhibition (C). To confirm this finding, RNA was isolated from RMF-EG cultured in 3D hydrogel followed by RT-qPCR gene expression analysis. RMF-EG in 3D hydrogels showed higher expression of *IL-8*, *MCP-1*, and *Col1a1* compared to 2D, subsequently reduced with DDR1 inhibition (D). * p<0.05, ** p<0.01, *** p<0.001 , **** p<0.0001.

Figure 1

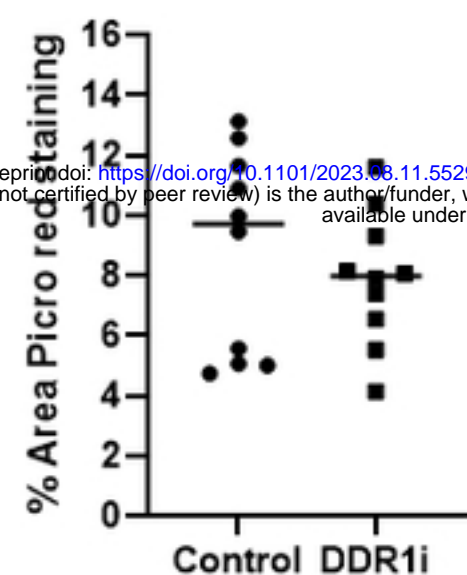
A



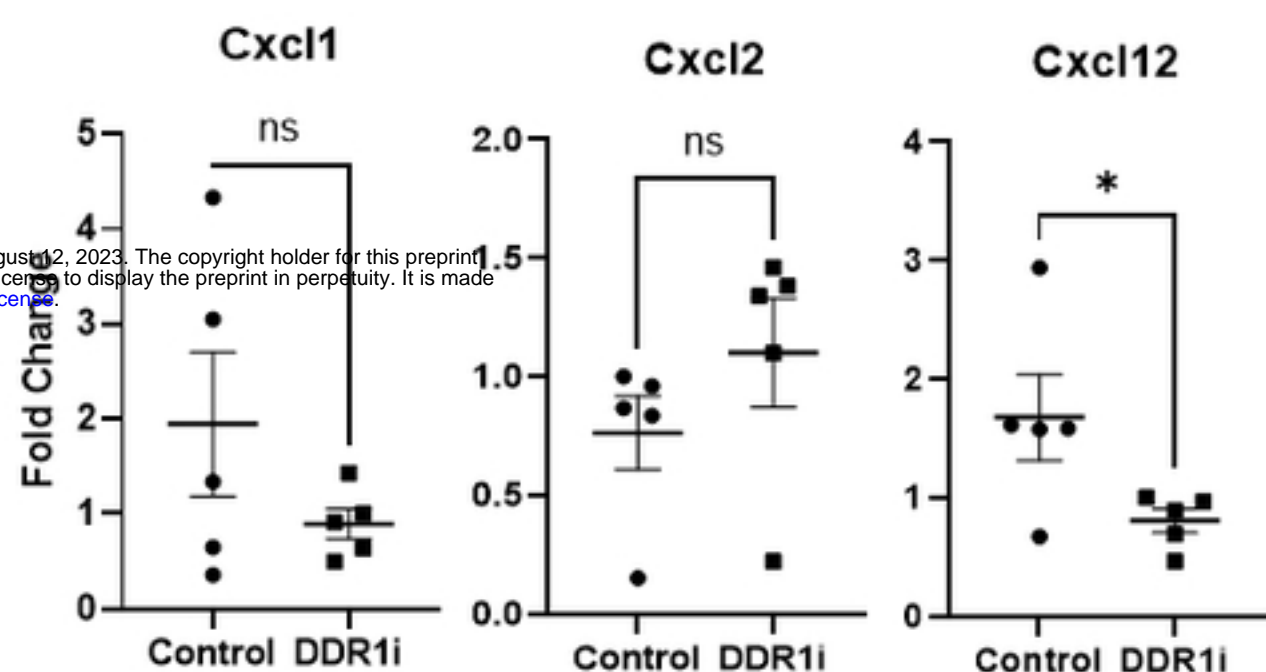
B



C



D



E

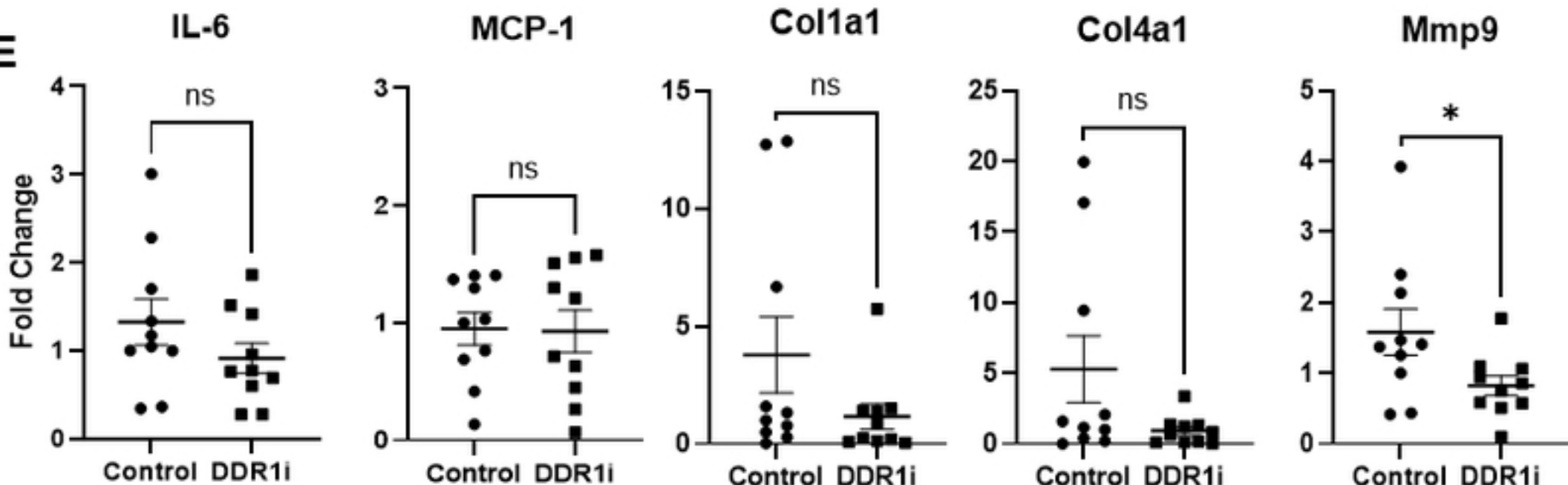


Figure 1

Figure 2

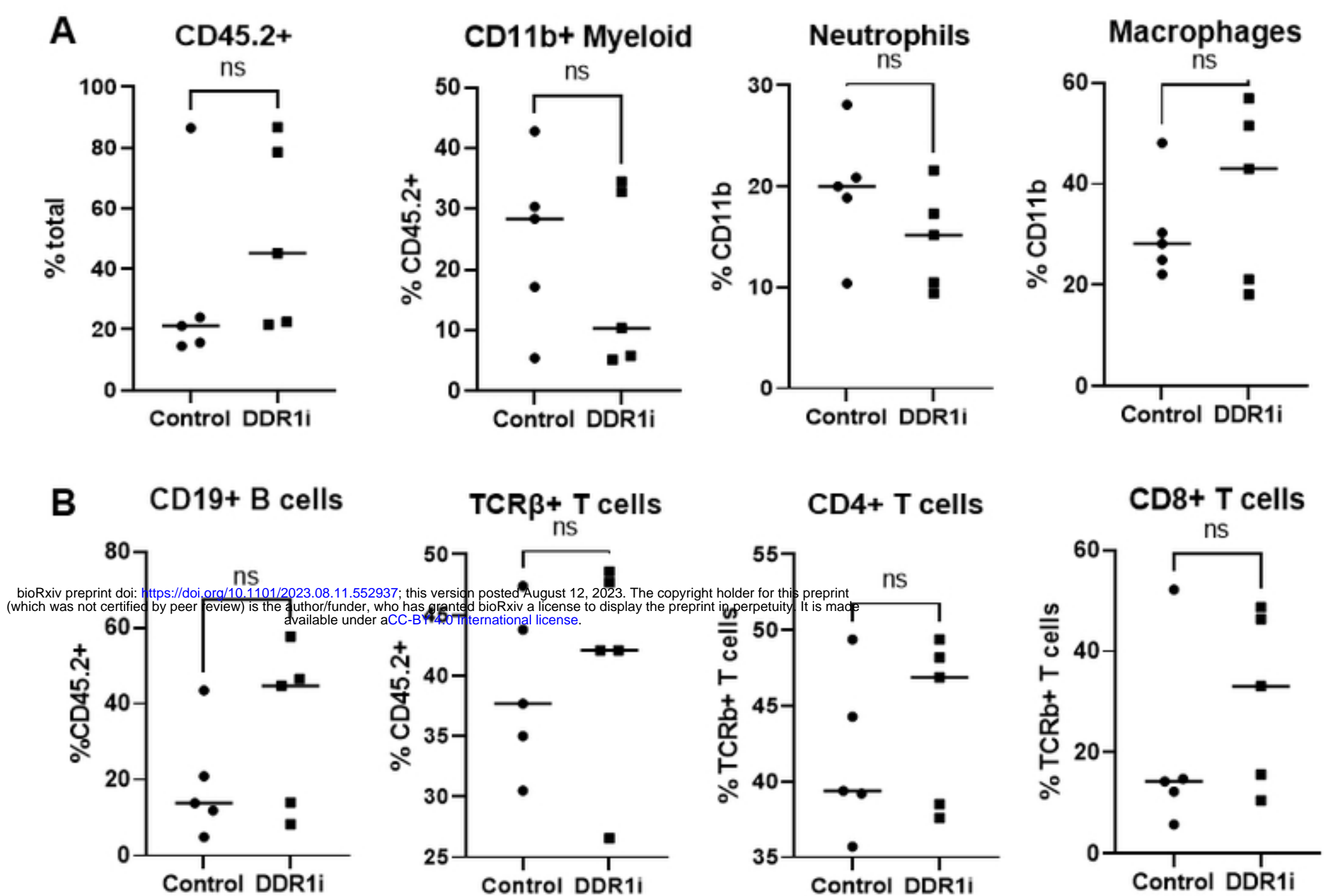


Figure 2

Figure 3

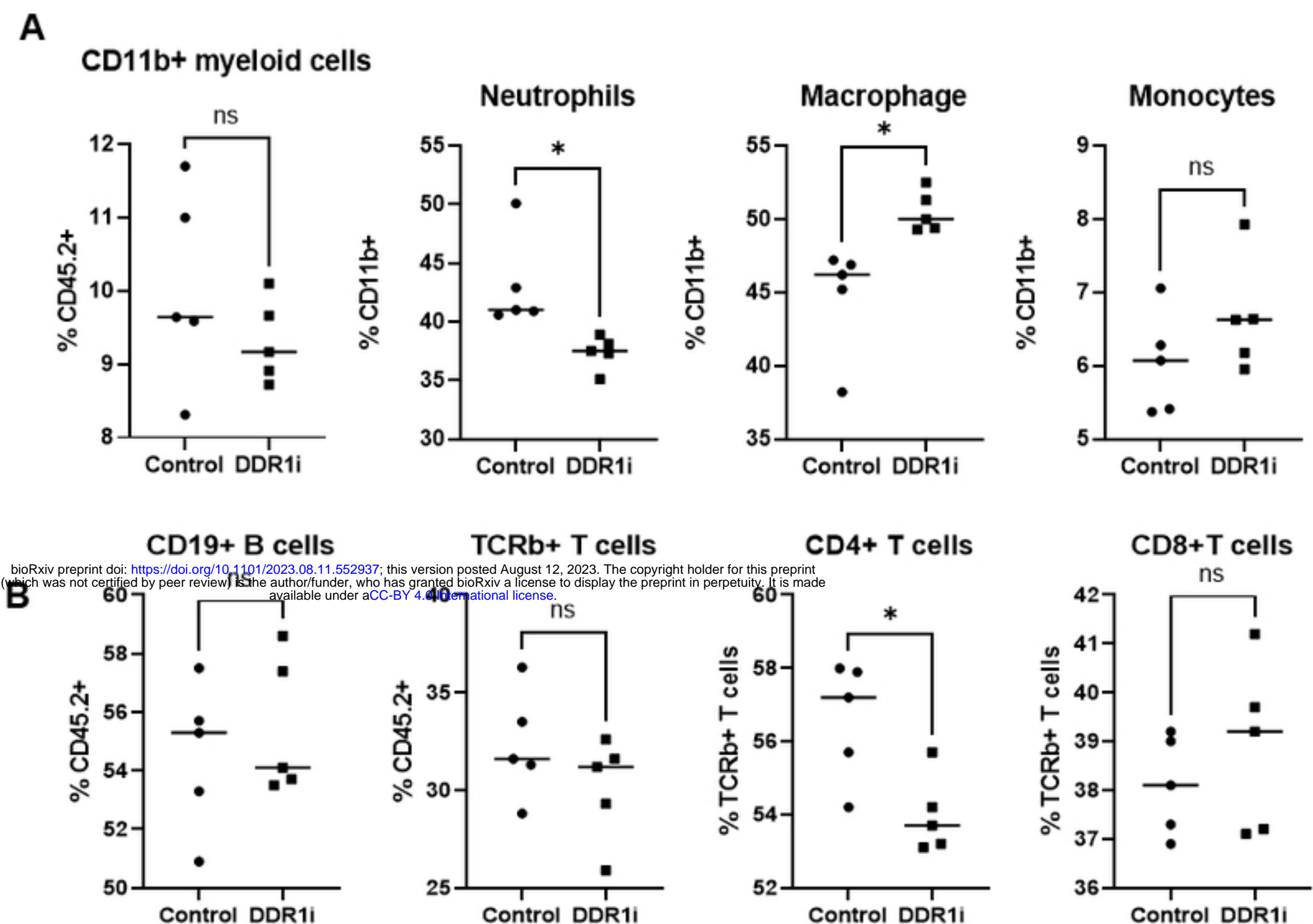


Figure 3

Figure 4

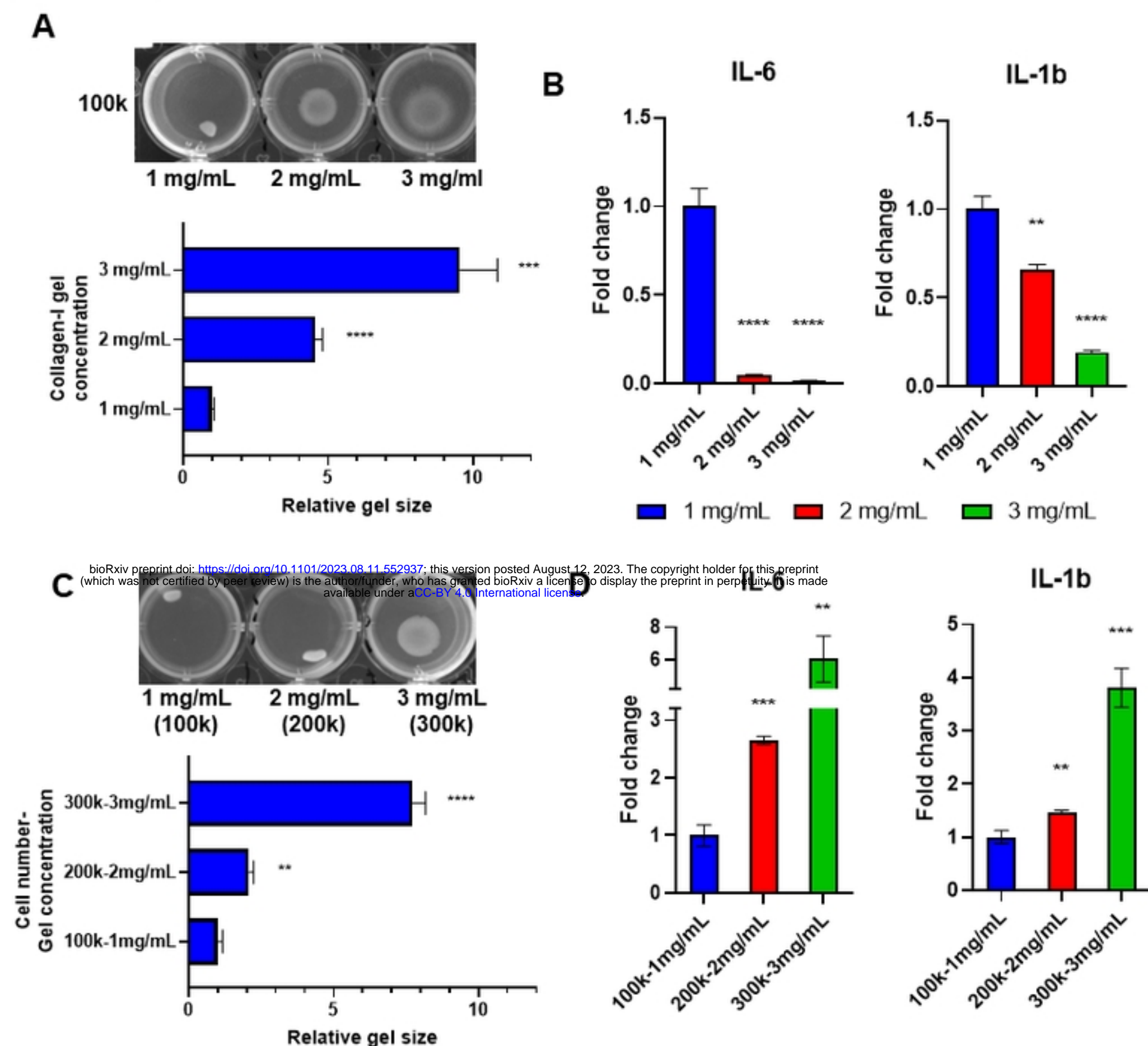
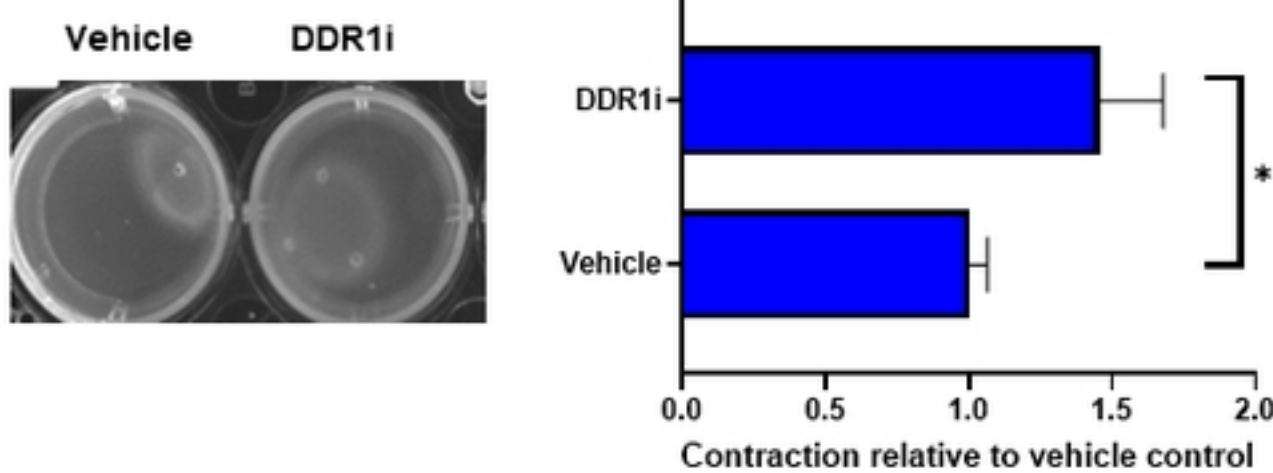


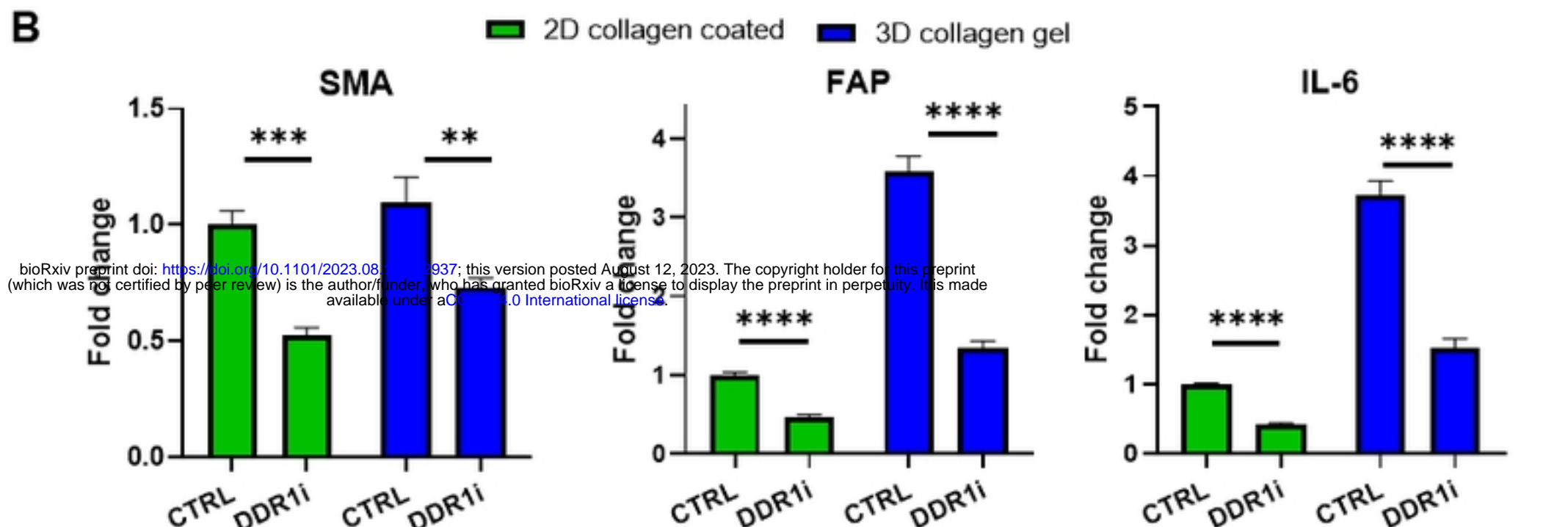
Figure 4

Figure 5

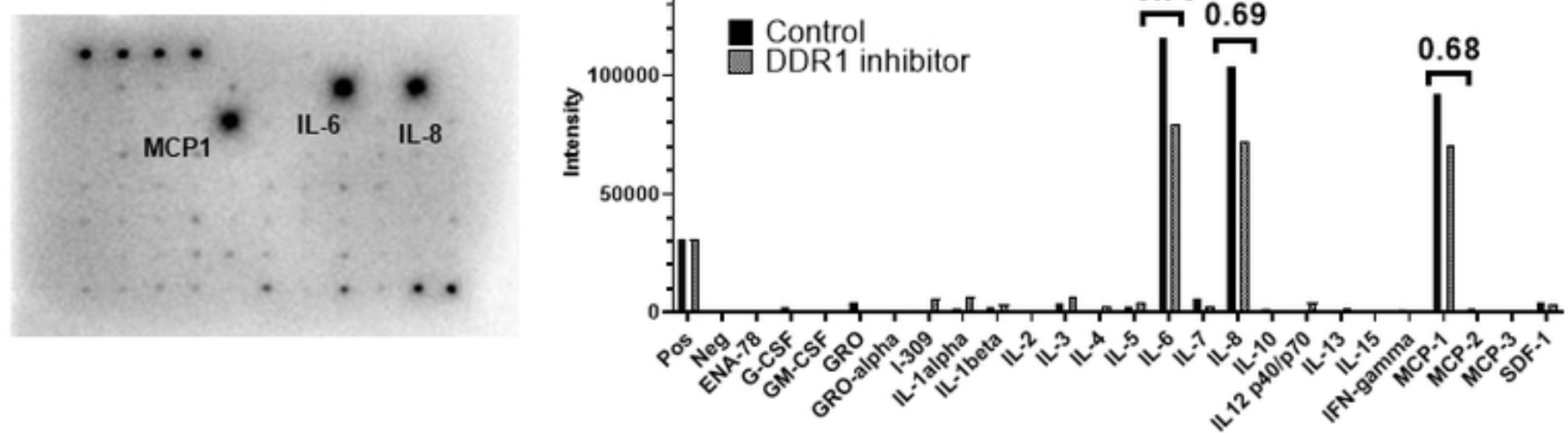
A



B



C



D

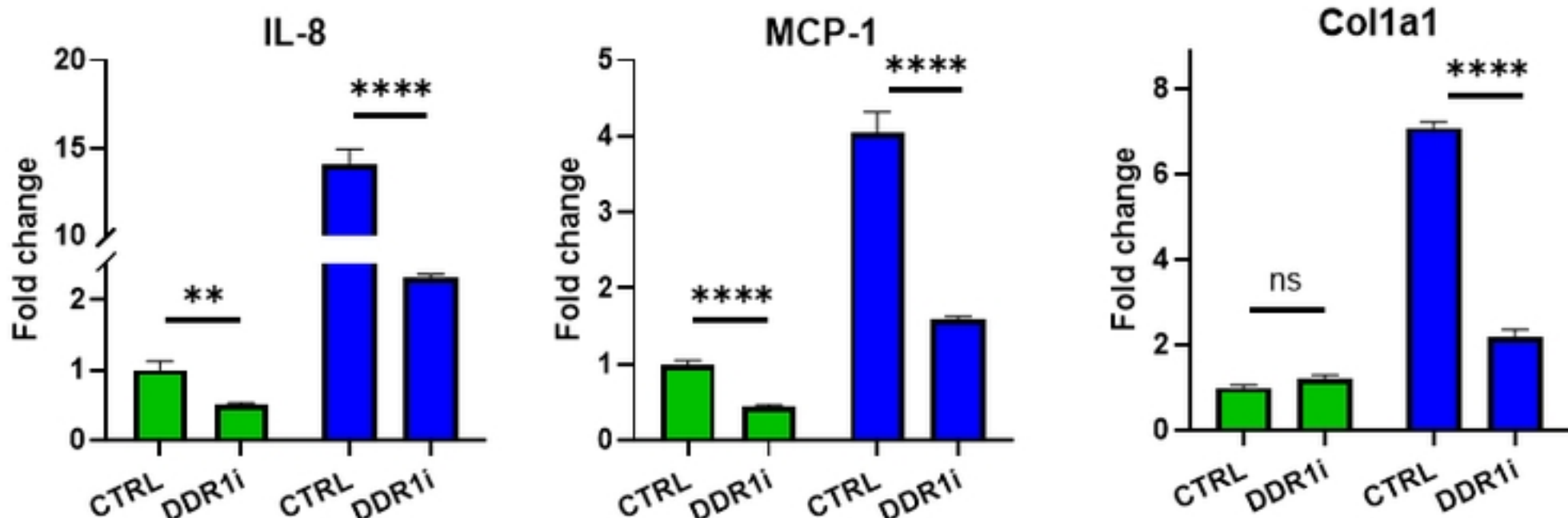


Figure 5

Figure S1 – Gating method for flow cytometry assessment of myeloid immune cell populations

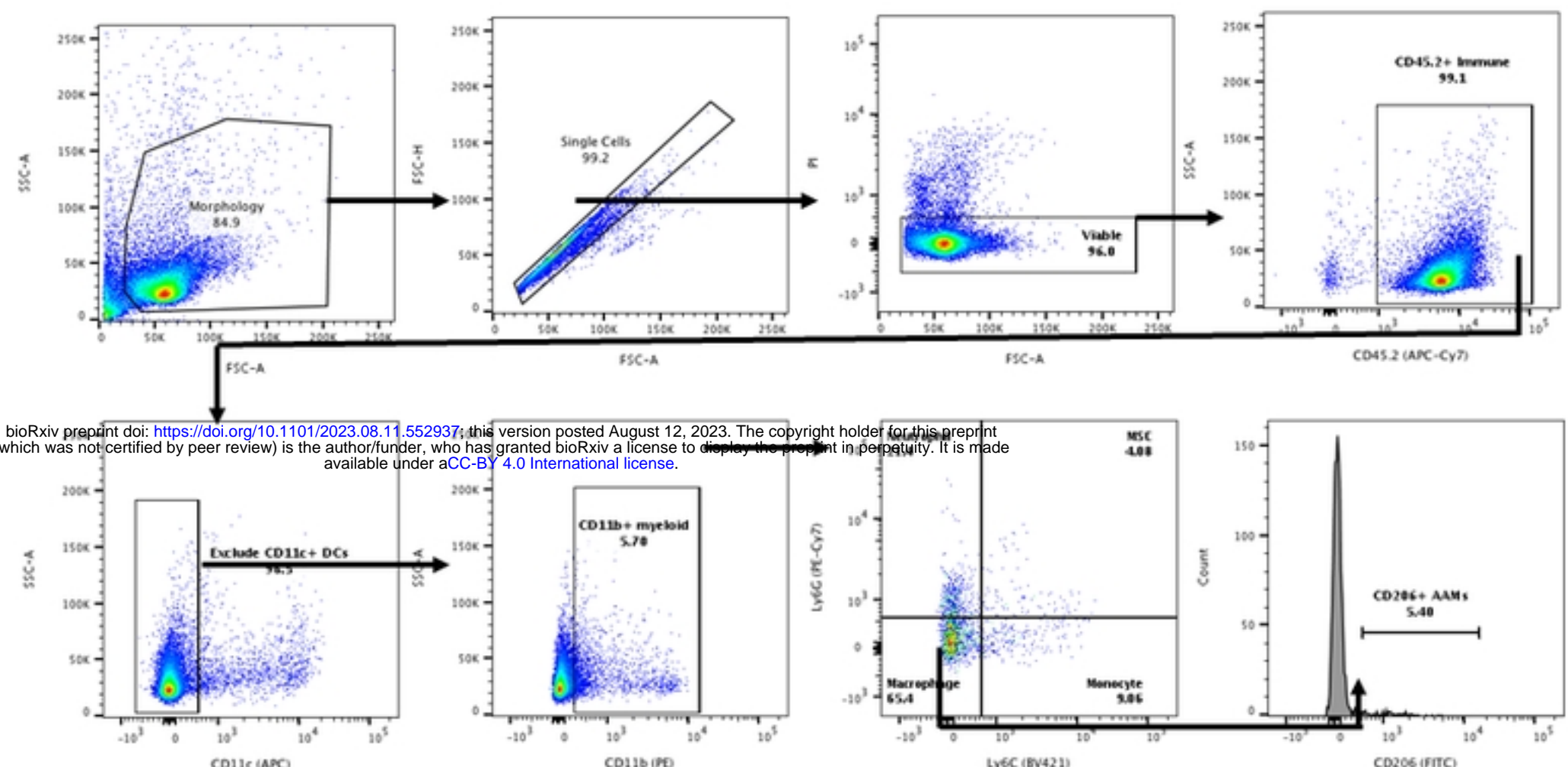


Figure S1

Figure S2 – Gating method for flow cytometry assessment of lymphoid immune cell populations

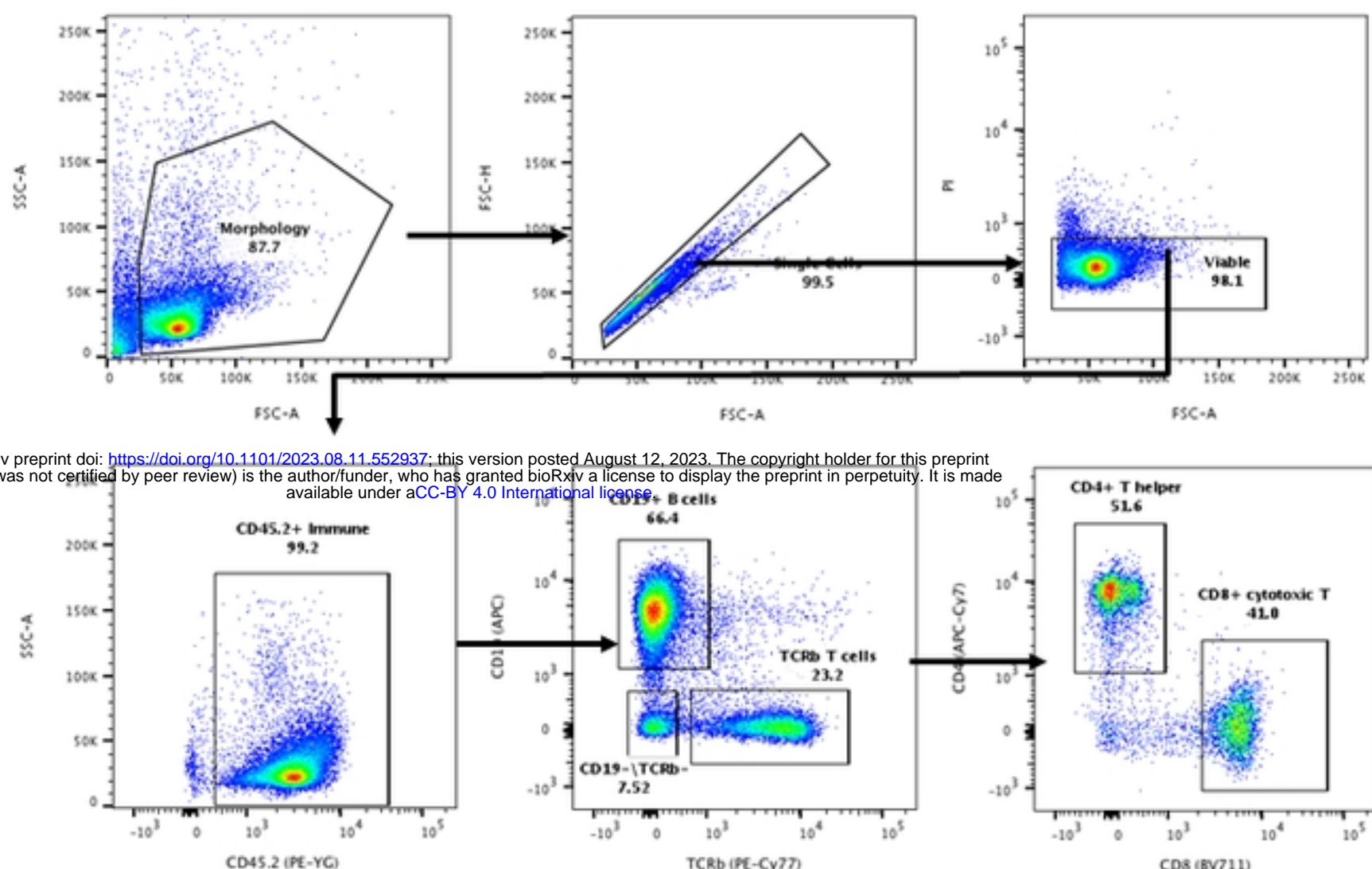


Figure S3- Dose titration of DDR1 inhibitors to assess cell viability and effective DDR1 inhibition

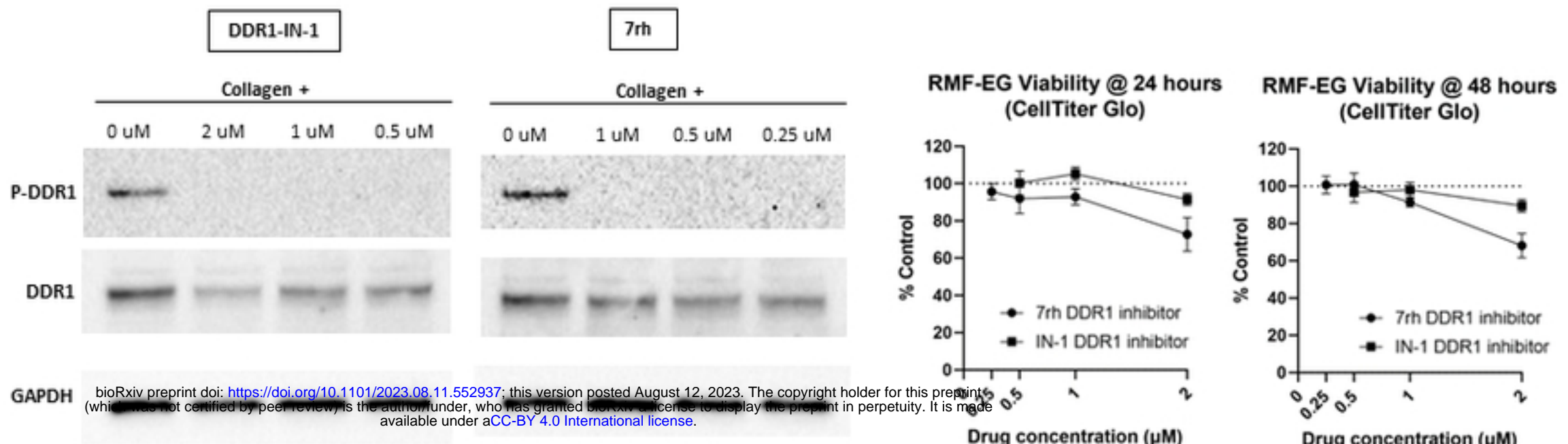


Figure S4 – Human multiplex cytokine array densitometry analysis of RMF-EG cultured in 3D collagen hydrogel, total cytokine assessment.

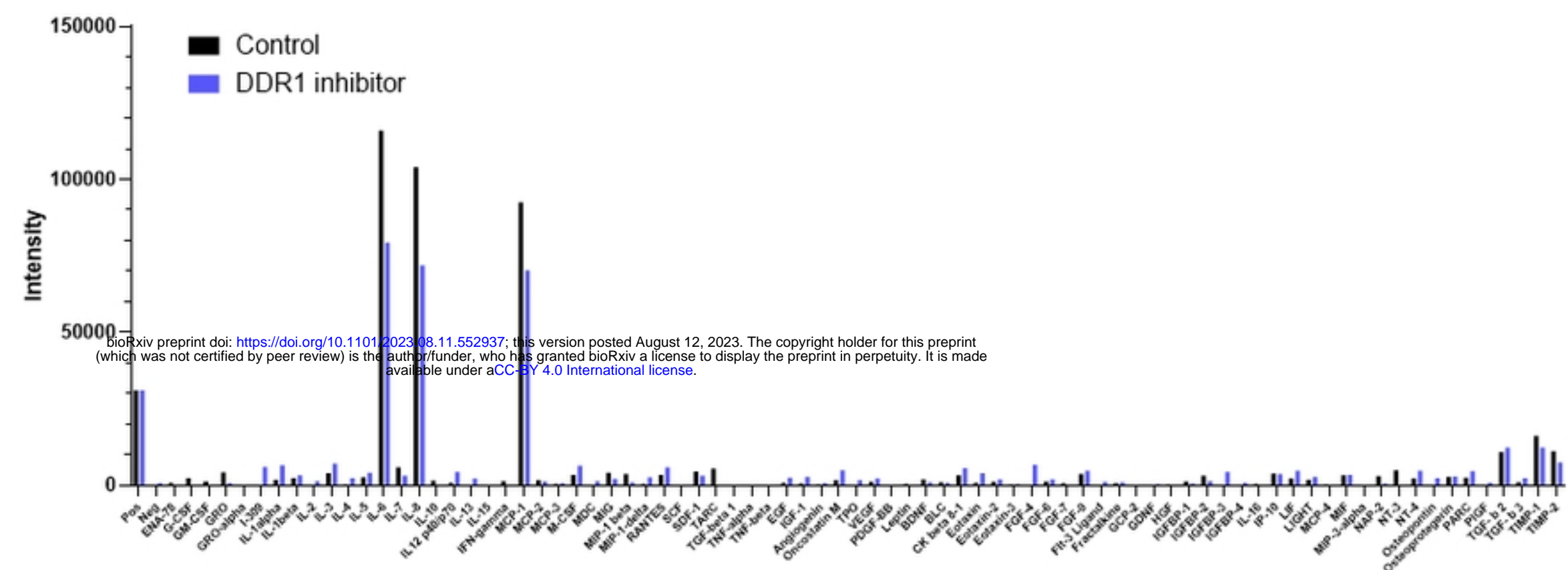


Figure S4

Figure S5- Assessment of SMA and IL-6 expression in RMF-EG cultured with recombinant TGF β 1 in the 2D or 3D context with (+) or without (-) DDR1i.

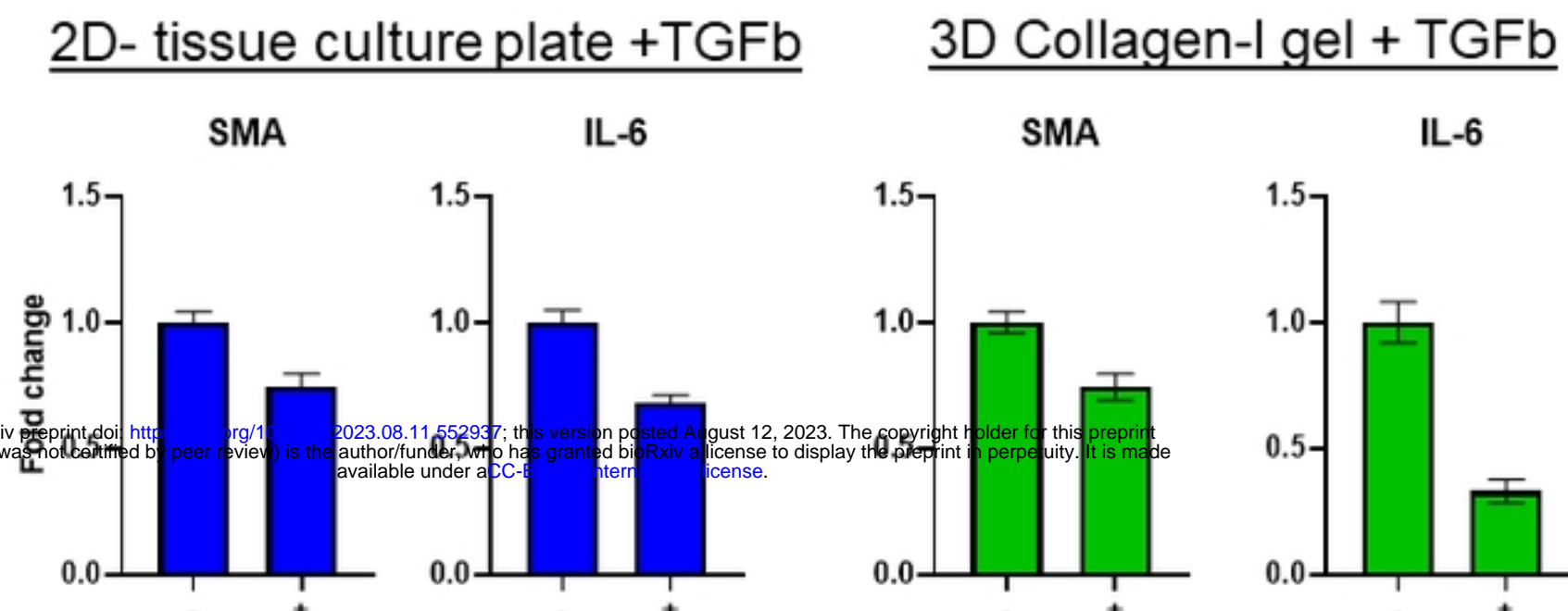


Figure S6- Effect of DDR1i on NF-κB signaling in RMF-EG

